EVIDENCE FOR LOW-INTENSITY D-D REACTION AS A RESULT OF EXOTHERMIC DEUTERIUM DESORPTION FROM Au/Pd/PdO:D HETEROSTRUCTURE

NUCLEAR REACTIONS IN SOLIDS

KEYWORDS: *neutrons, protons, DD reaction, Pd heterostructure, nuclear detection, deuterium, hydrogen, deuterium diffusion*

A. G. LIPSON* and B. F. LYAKHOV *The Russian Academy of Sciences*
Institute of Physical Chemistry, 31 Leninsky Prospect, 117915 Moscow, Russia

A. S. ROUSSETSKI *The Russian Academy of Sciences*
Lebedev Physics Institute, 117924 Moscow, Russia

T. AKIMOTO and T. MIZUNO *Hokkaido University*
Department of Nuclear Engineering, Sapporo 060, Japan

N. ASAMI, R. SHIMADA, and S. MIYASHITA
New Hydrogen Energy Laboratory, Institute of Applied Energy
Sapporo 004, Japan

A. TAKAHASHI *Osaka University*
Faculty of Nuclear Engineering, Osaka 565, Japan

Received July 19, 1999
Accepted for Publication December 22, 1999

Low-intensity nuclear emissions (neutrons and charged particles) due to exothermic deuterium desorption from Au/Pd/PdO heterostructure loaded with deuterium by electrolysis have been studied by NE213 neutron detection as well as SSB and CR-39 charged-particle detectors in low-background conditions with large statistics. Similar measurements were performed with the Au/Pd/PdO:H heterostructure as a control. It has been established that in experiments with the Au/Pd/PdO:D system, the excessive 2.45-MeV neutrons and 3.0-MeV protons are better detected than with the Au/Pd/PdO:H system, where those detection rates for n and p did not exceed the cosmic background level. The levels of neutron and proton emissions for 40- to 60-μm-thick samples are found to be close to one another and after subtracting background (Au/Pd/PdO:H count rate) consist of $I_n = (19 \pm 2)\cdot 10^{-3}$ n/s and $I_p = (4.0 \pm 1.0)\cdot 10^{-3}$ p/s in a 4π solid angle, respectively. These yields of D-D reaction products in Au/Pd/PdO heterostructure comply with the mean D-D reaction rate of $\lambda_{dd} \sim 10^{-23} s^{-1}$ per D-D pair.

I. INTRODUCTION

The problem of lattice-induced nuclear reactions (LINRs) or the existence of so-called cold fusion is still open. Despite 10 yr of the intense efforts of many research groups in various countries, there are no convincing nuclear data that would confirm generation of D-D reactions in solids at room temperature. In dozens of such experiments on neutron and charged-particle detection, the problem of the very low intensity of the observed emissions has been complicated by total irreproducibility of nuclear results.[1–3] Very often, results obtained in one place could not be replicated in another. Note that

*Also affiliated with New Hydrogen Energy Laboratory, Institute of Applied Energy, Sapporo 004, Japan.

the presence and reproducibility of nuclear emission in deuterated solids depend at least on (a) the type of material and crystalline structure of samples,[4] (b) the manner of sample excitation (electrolysis, gas loading, phase transitions, strain, fracture, temperature change, etc.),[1–5] (c) the thermal neutron background condition,[6,7] (d) the purity of the D used,[8,9] etc.

All these features of LINR allow the formulation of this phenomenon as follows. Under these terms, LINR (with respect to D-D reaction) could be regarded as an anomalous (in terms of conventional nuclear processes in vacuum), random, and rare nuclear effect in a crystalline lattice of essentially nonequilibrium deuterated solids, which are induced by sharp changes in their structure, i.e., phase transitions, D loading, mechanical strains, etc. In these circumstances, the LINR might be caused by gigantic fluctuations of elastic energy in a crystalline lattice. Accordingly, to generate a D-D type of nuclear reaction in a Pd lattice, a principal condition could be the creation of large fluctuations of elastic energy in the sample and/or high screening potential for a deuteron Coulomb barrier. In terms of elastic energy fluctuations, it is implied that it is necessary to introduce a high concentration of nonequilibrium phonons in a crystalline lattice, which can produce a phonon-laser effect[10] (creation of multiphonon excitations). For instance, such phonons could be generated in the process of exothermic D desorption[11–13] from the specially prepared Pd heterostructures loaded with D during their spontaneous and induced deformations with or without heating.

In 1992, a Au/Pd/PdO heterostructure was developed and studied at the Institute of Physical Chemistry of the Russian Academy of Sciences (IPS/RAS) in Moscow. It possesses a high D capacity at electrochemical loading, and D transport in this kind of heterostructure is more intense than in pure Pd foils due to the very high mobility of deuterons at the Pd-PdO interface.[11] During spontaneous deformation accompanying the fast exothermic D desorption, this heterostructure demonstrates neutron emission (measured by BF_3 proportional detectors).[12] With external deformation applied to the samples, the neutron emission character became more uniform and reproducible.[13] Later, the observation of charged particles in a similar heterostructure system was reported.[14]

Recently, at a low-energy deuteron implantation ($2.5 < E_d < 10$ keV) in a Au/Pd/PdO heterostructure, the highest screening potential, $U_s = 600$ eV, was observed,[15] which also indicates the excellent conditions for deuteron screening in these kinds of samples, despite a small loading ratio ($x = \mathrm{D/Pd} = 0.13$). At the same time, for instance, Ti metal with a very high loading ratio ($x = \mathrm{D/Ti} = 3.76$) demonstrated a very low screening potential,[16] close to that for a D gas target [several tens of electron volts (Ref. 17)], while for Pd metal foils the screening potential ($U_s = 250$ eV, $x = \mathrm{D/Pd} = 0.23$) is much higher than for Ti but still lower than for a heterostructural target. The Ref. 15 results mean that a maximal D-D reaction enhancement at very low deuteron energy should be expected for a Au/Pd/PdO:D heterostructure compared to other metal-deuteride systems, including pure Pd.

It is important to emphasize that D (H) desorption in Au/Pd/PdO:D heterostructure samples is essentially an exothermic process in spite of the weakly endothermic character of H desorption from pure Pd metal. The main cause of exothermic H desorption in a Au/Pd/PdO:D sample is the presence of a PdO layer at the surface, because Pd oxide acts as a catalyst for the strongly exothermic $H + H \rightarrow H_2$ reaction. Moreover, the Gorsky effect[11] that induces D transport to the PdO surface due to mechanical strain also makes it possible to decrease a surface barrier for D desorption and in this way to remove endothermicity of the desorption process in a heterostructure.

In this paper we show the results of D-D neutron and proton measurements carried out during spontaneous and induced deformations following exothermic D desorption in a thin Au/Pd/PdO:D heterostructure loaded with D by electrolysis. We demonstrate that in experiments with the Au/Pd/PdO:D system, excessive 2.45-MeV neutrons and 3.0-MeV protons are detected, as compared to the Au/Pd/PdO:H system, where detection rates for neutrons and protons did not exceed the cosmic background level. The levels of neutron and proton emission are found to be the same order of magnitude, and after subtracting background (Au/Pd/PdO:H count rate), they are equal to $I_n = (18.5 \pm 0.18) \times 10^{-3}$ n/s and $I_p = (4.0 \pm 1.0) \times 10^{-3}$ p/s, respectively, in the 4π solid angle.

II. EXPERIMENTAL TECHNIQUE AND METHODS

II.A. Sample Preparation and Characterization

The Au/Pd/PdO heterostructure samples with thicknesses of 8 to 300 μm (typical area $S = 45 \times 20$ mm^2) used in our experiments[12,13] were produced at IPS/RAS. The 99.99% pure cold-rolled Pd foils[a] that were taken for sample production, before manufacture of the heterostructure, had been subjected to annealing in vacuum ($p = 10^{-7}$ Torr) at temperature $T_a = 1273$ K for 5 h at a heating rate of 10 K/min and cooling rate of 1.5 K/min. To form an oxide layer on the foils' surface, they were heated in an oxygen flame (by propane-oxygen torch at $T_h \approx 1220$ K) for 5 to 10 s. As a result, a carbon-containing thin oxide layer of PdO_xC_y ($x \sim 0.57$, $y \sim 0.08$, in accordance with secondary ion mass spectrometry data) having a gray or, sometimes, pink color with a thickness of $\sim 35 \pm 10$ nm was created on both sides of the Pd foils. After this procedure, one side of the PdO/Pd/PdO heterostructure obtained was covered by a "Teflon mask"

[a] From Nialco Corporation.

[polytetrafluoroethylene (PTFE) lacquer], and a 0.1-μm-thick gold coating was deposited on the sample's free side by an electrochemical technique. The deposition of Au on the PdO free surface was carried out with the standard cyanic electrolyte for gold plating[13] that does not contain iron group metals and organic lustre agents. The current output of the deposition process is ~100%, which excludes a H evolution at the PdO surface and, thus, prevents a possible PdO reduction. After finishing the Au/Pd/PdO heterostructure preparation, the samples produced underwent final annealing in vacuum at 573 K (after PTFE lacquer mask removal with acetone) to remove possible volatile contaminants that could be sorbed by samples during preparation.

To load heterostructure samples with D or H (in blank experiments), the electrochemical method was applied. Electrolysis was carried out in a special glass cell with cathodic and anodic spaces separated to prevent O contact with the cathode during electrolysis. The electrolyte was a 1 M solution of NaOD in D_2O or 1 M NaOH in light water, a Pt sheet was used as an anode. Electrolysis time, depending on the sample thickness, varied from 5 min for 8-μm samples to 90 min for 300-μm ones at direct current density of 20 mA/cm^2. A golden ohmic electrical contact has been used for electrolytic loading of heterostructure samples. To prevent a voltage drop across the ohmic contact, it must not be immersed in electrolyte during the loading procedure. Under the electrolysis conditions used, the mean loading ratio in the samples after completion of electrolysis, determined by both thermal desorption and anodic polarization techniques, was approximately $x = \mathrm{D/Pd} = 0.70$ (if normalized to the total volume of the sample). Immediately after electrolysis, the samples were removed from the cell, washed in pure heavy (or light) water, slightly dried (to prevent thermal flash), and fixed in the sample-holder. The elapsed time between the electrolysis rapture and the start of nuclear measurements was usually ~1 to 2 min. For neutron and CR-39 track detector measurements in air atmosphere, a special sample-holder was designed that allowed tight compression of the Au/Pd/PdO:D(H) samples (in the normal direction toward the large face of the sample) and, thus, produced essential strain in them (~20 MPa). In this case, self-heating of samples was achieved during their exposure in air atmosphere due to D (H) exothermic desorption heat and recombination of D molecules with O. After long-term strain, the D desorption from the samples has a non-uniform character with a mean rate of $\langle v_{\mathrm{D}} \rangle \sim 10^{16}$ to 10^{17} at.D/s·cm^2. After 20 h of mechanical loading, the residual D concentration in the sample at room temperature ($T = 290$ K) was found to be ~10% of its initial value.

In the case of charged-particle measurements in vacuum, the samples were fixed in a stainless steel sample-holder at both ends by clamps (quasi-spontaneous deformation regime). In background runs carried out for the same experimental day before or after the foreground one, the Au/Pd/PdO samples (that had no prior contact with D) with H were loaded.

II.B. Neutron Measurement System

To detect neutrons from the cell with compressed Au/Pd/PdO:D (H) samples, two separate 5-in. NE-213 liquid-scintillator detectors were installed at a distance of 24 cm from each other (Fig. 1). To decrease a natural neutron background, the detectors were surrounded by boron-containing polyethylene, and the entire setup was placed in the underground laboratory of Hokkaido University under 10 m of heavy concrete. Because of this underground shielding, a one-order-of-magnitude decrease in neutron background was achieved as compared to ground-level conditions.

To increase the accuracy and reliability of neutron spectra measurements, the high-gain (system 1) and low-gain (system 2) methods have been used simultaneously for neutron detection. The high-gain system is operated in the 0.8- to 3.5-MeV range of proton recoil edge, while the low-gain system is between 1.0 and 7.1 MeV. To exclude detection of gammas during neutron detection, the pulse-shape analyzer was used, which allowed a high level of confidence in separating gamma and neutron pulses. To prevent uncontrolled electromagnetic noise signals via ground circuit, a noise cut transformer was introduced to the power supply input.

The energy scale calibration of both detectors was carried out with a ^{22}Na standard gamma source by determining the proton-recoil distribution. The effective neutron energy corresponding to the proton edge was calculated on the basis of the known response functions of detectors.[18,19]

Neutron-energy calibration of the detectors as well as determination of detector efficiency was carried out with a ^{252}Cf neutron source with intensity $I = 2.0 \times 10^3$ n/s in the 4π solid angle, which was installed in the sample position (between the two detectors). The distributions of a number of proton recoil pulses versus neutron energy in logarithmic coordinates have a quite uniform linear character as a smooth function, diminishing with neutron energy increase, for both detectors (Fig. 2). This fact indicates that the detection systems adjustment and operation are adequate for taking low-background spectral measurements and detection of 2.45-MeV (D-D) neutrons. The efficiency of measurements in reference to fast neutrons is as follows: for system 1, $\epsilon_1 = 4.8\%$; for system 2, $\epsilon_2 = 5.1\%$. In energy intervals corresponding to the 2.45-MeV neutron peak location (2.0 to 3.0 MeV), the efficiencies were $\epsilon_1' = 4.0\%$ and $\epsilon_2' = 4.7\%$. Therefore, the total efficiency of neutron detection for a couple of detectors used in the energy interval of interest is ~9%. We must emphasize that the detector efficiency and neutron background condition used allow an increase in sensitivity with respect to 2.5-MeV neutrons in our experiment by at least one order of magnitude compared to

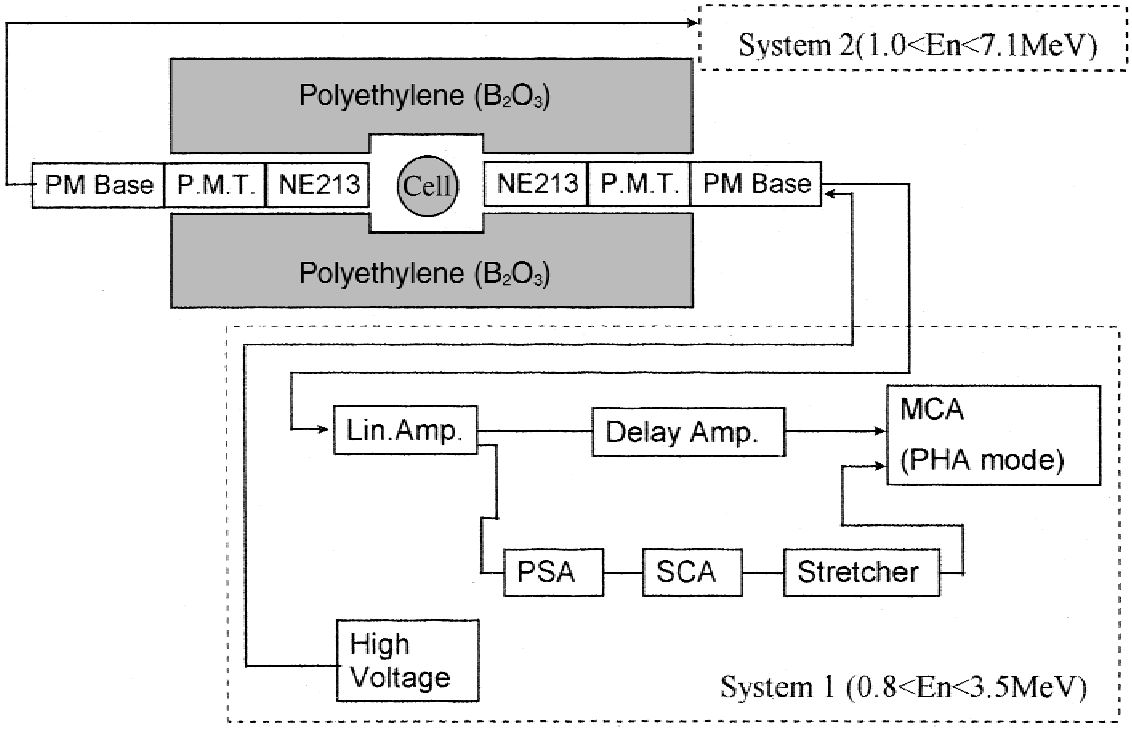

Fig. 1. The NE-213 neutron detection facility.

previous well-known spectral neutron measurements[2,3] in metal-deuterium systems.

II.C. Charged Particle Detection Systems

II.C.1. SSB Measurements

Measurements of the total spectra of charged-particle emission were carried out for samples with thickness from 40 to 60 μm at the Department of Nuclear Engineering of Osaka University. A vacuum setup, which is shown in Fig. 3, was used also with an electromagnetic noise suppression system. The distance between the SSB detector window and the sample surface was fixed at $x = 1.0$ cm. The ORTEC SSB detector (thickness $h = 150$ μm, area $S = 100$ mm^2) had a discrimination threshold of ~100 keV to eliminate low-amplitude noise signals. Typical background spectra (Fig. 4) for ~1 week of continuous observation have sharply decreasing shape versus energy and generally do not contain events with energies higher than 7.7 MeV. The background count rate in the energy interval of interest (1 to 4 MeV) in which D-D protons have been expected is very low and has not exceeded 0.15 count/h. The detector efficiency determined with a ^{241}Am alpha source installed in the sample position was 3.4%.

To establish the thickness dependence of 3-MeV proton yield, a special series of measurements with samples between 8 and 300 μm thick were carried out in the proton spectral range from 2.5 to 3.5 MeV. To this end a high-efficiency ($\epsilon = 12\%$) ORTEC SSB detector with a large surface area ($S = 900$ mm^2, $h = 150$ μm) has been used at the New Hydrogen Energy Laboratory in vacuum conditions similar to those used for total spectrum measurement.

After loading, washing, and drying, the sample was fixed at both ends in a stainless steel sample-holder (Fig. 3) by clamps. The sample-holder was provided with a heater that allowed heating the samples up to 373 K at a rate of ~5 K/min in the linear regime. The typical duration of sample exposure was ~3 to 5 h at $T = 300$ K in background runs (with Au/Pd/Pd:H samples) as well as in foreground ones. Owing to intensive D desorption, the pressure in the vacuum chamber was constant at a level of ~10^{-2} Torr during the measurements.

II.C.2. Application of CR-39 Track Detector

To confirm the results of SSB measurement and to check the yield of D(d, p)T reaction, an independent CR-39 track detector technique has also been applied to detect charged particles. To improve the accuracy of CR-39 detection, we searched simultaneously for tracks of 3.0-MeV protons and 1.0-MeV tritons that are both the products of the D(d, p)T reaction. To this end we detected solely double proton-triton (pt) events, consisting of 3-MeV proton and 1.0-MeV triton tracks, respectively, which could be emitted from the same space point

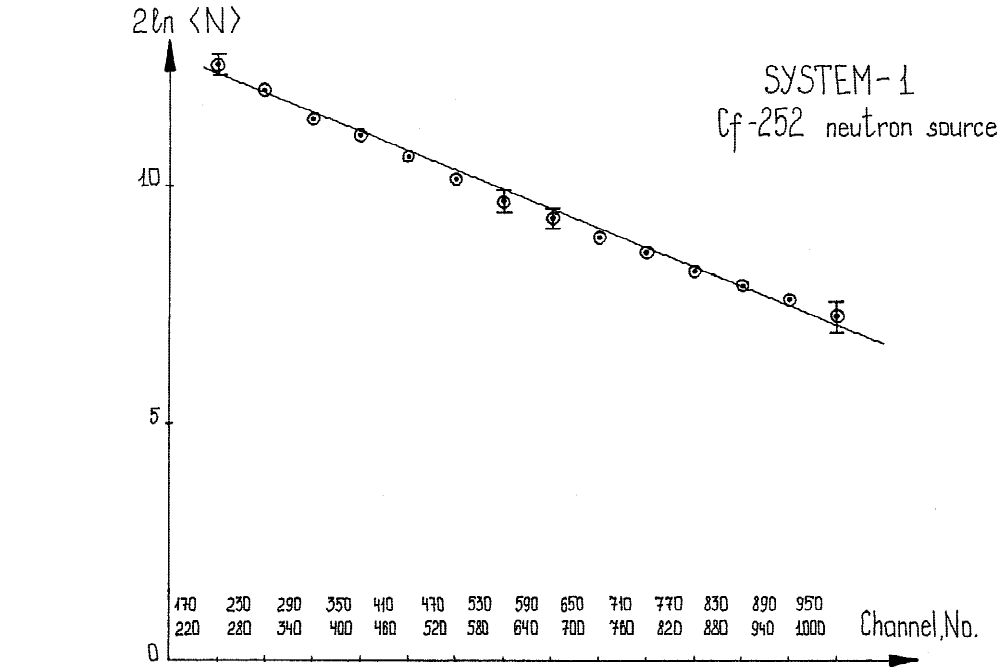

(a)

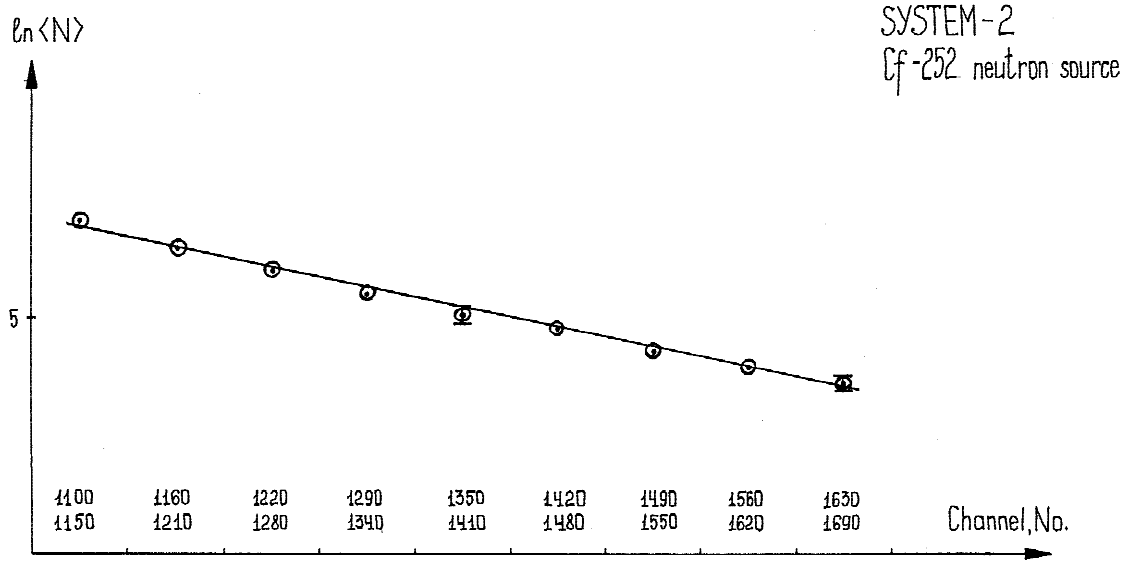

(b)

Fig. 2. Distribution of proton recoil pulses as a function of neutron energy with a ^{252}Cf neutron source (a) for the high-gain system, system 1 and (b) for the low-gain system, system 2.

of the heterostructure surface, i.e., as a result of different D-D reaction.

In the CR-39 experiments the 30-μm-thick heterostructure samples of PdO/Pd/PdO:D(H) and detectors with dimensions 4×2 cm^2 have been used. After the D loading procedure, the sample was tightly fixed on the surface of the CR-39 detector by a sample-holder similar to those used in neutron measurement. The sample attached to the detector was subjected to temperature cycling from room temperature to 323 K and spontaneously cooled back during a 1-h period.

The calibration of CR-39 detectors by D-D reaction products was carried out with a high-current low-energy deuteron generator in the Laboratory of Nuclear Science of Tohoku University (Sendai, Japan). The yield of the $D(d, p)T$ reaction from the TiD_2 target under

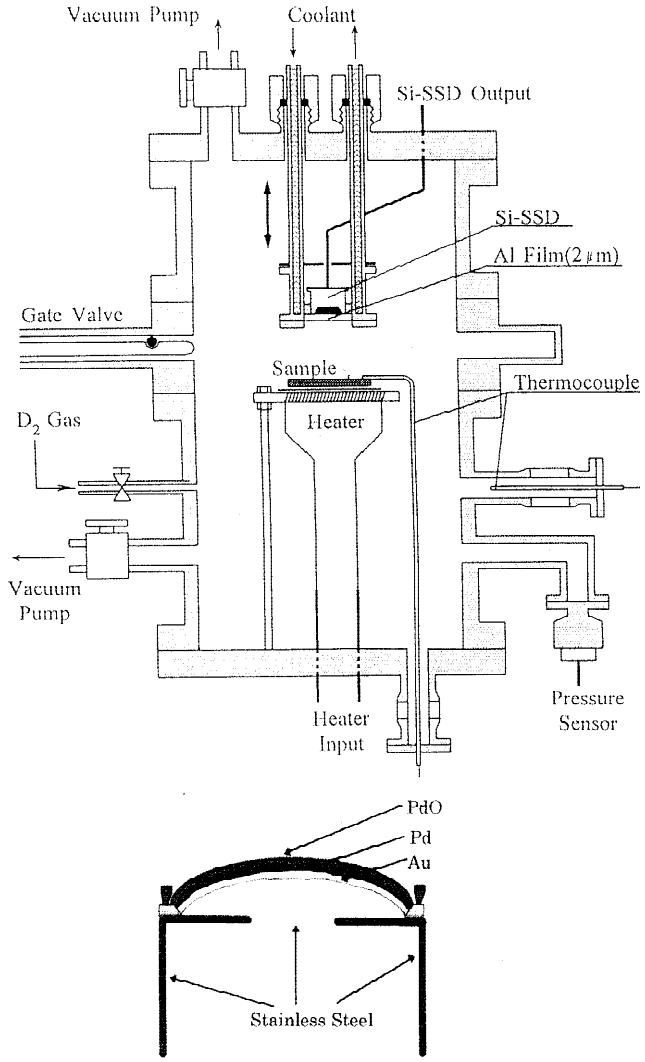

Fig. 3. Vacuum setup for SSB charged-particle detection. In insert the arrangement of Au/Pd/PdO:D(H) heterostructure sample is presented.

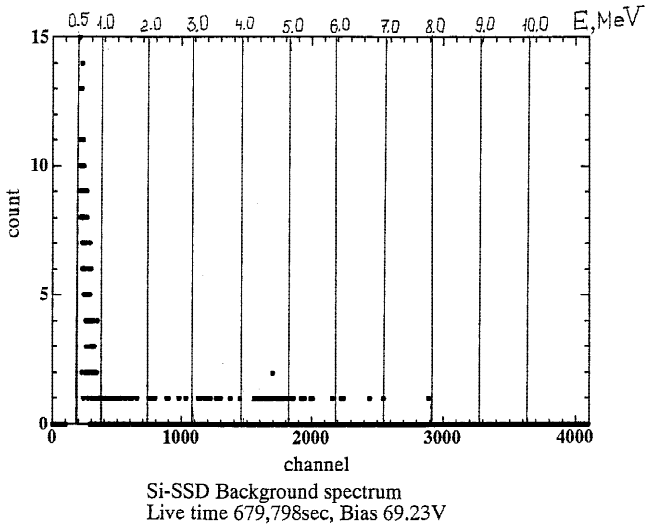

Fig. 4. Typical charged-particle (natural) background spectrum obtained for a long detection time (~1 week) at Osaka University.

bombardment with a 10-keV deuteron beam has been used for calibration experiment. In accordance with calibration measurement (Fig. 5a), the track diameters of protons and tritons from the D(d, p)T reaction taking place in the thin target layer of 0.1 μm are ~5 and 7 μm, respectively.

To obtain track width distribution, the CR-39 plates have undergone an etching procedure in a 6 M solution of NaOH for 7 h at T = 343 K. The track diameters were measured with an MBI-9 microscope. The choice of proton and triton tracks generated in the same surface sites (pt events) has to be in accordance with the following criteria:

1. Tracks with a clear circular or oval shape must have diameters of 5.0 to 5.5 μm for protons with energy between 2.5 and 3.0 MeV, and 6.5 to 7.5 μm for tritons with energy between 0.5 and 1.5 MeV.

2. The centers of these tracks must be located at a distance <16 μm, in accordance with maximum divergence of proton and triton tracks generated in the D-D reaction, which are emitted from the same point on the sample surface, taking into account critical detection angles for these particles in CR-39 detectors.[20]

The micrographs of several possible candidates for double pt tracks, which satisfied criteria 1 and 2, are presented in Fig. 5b. Taking into consideration the critical angles[20] for 3.0-MeV protons (Θ_p = 30 deg) and 1.0-MeV tritons (Θ_t = 50 deg) in CR-39, the efficiency of the simultaneous detection of pt events by the CR-39 track detector used has been evaluated as ϵ_{pt} = 4.7%.

III. EXPERIMENTAL RESULTS AND DISCUSSION

III.A. Neutron Measurements

The total measurement time of the 50 foreground runs was ~1×10^6 s, and for 50 backgrounds, ~8×10^5 s. The duration of a run in background and foreground varied from 2000 to 60 000 s. The total differences in intensities of emission in foreground and background runs and full expected errors for different spectral intervals were calculated separately for high- and low-gain systems in accordance with "combination of independent measurements with unequal error."[21] In Fig. 6 a typical sequence of neutron detection during one experimental day, including background and following foreground run, is presented. In the background run (Au/Pd/PdO:H sample) one can see only events (counts within 50-s duration) that did not exceed the level of three standard

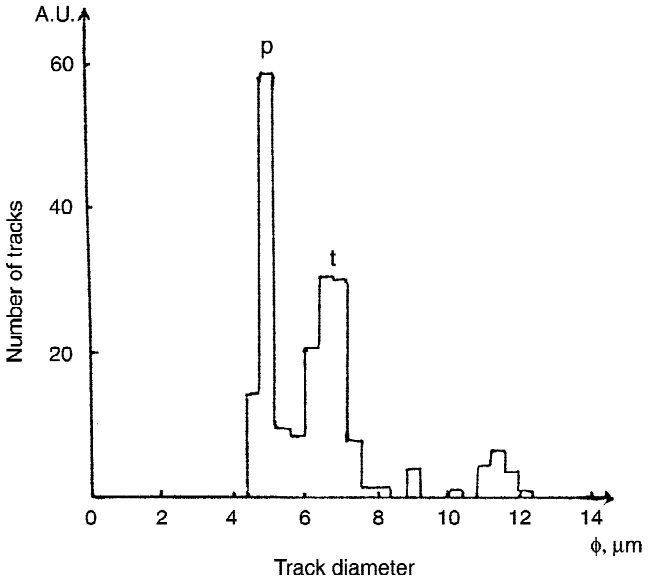

Fig. 5a. Distribution of track diameters for charged particles ($p, t,^3$He) from the D-D reaction, obtained during the calibration procedure with CR-39 track detectors.

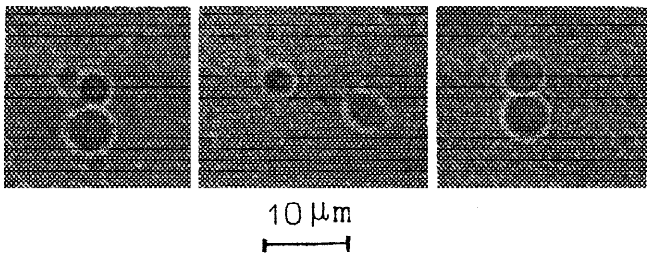

Fig. 5b. The micrographs of three possible candidates for pt double tracks, which satisfy the criteria of the D(d, p)T reaction observation.

deviations. At the same time, in the foreground that was measured just after the background run, three events were observed with a statistical significance of more than four standard deviations above the mean error level. The neutron emission as a function of time usually has a nonuniform character (as well as D desorption); however, an excess above background level was observed for 10 to 15 h for 60-μm-thick samples.

Comparison of neutron spectra obtained during all background and foreground runs for both the high- (Fig. 7a) and low-gain (Fig. 7b) independent systems demonstrates a significant excess in the count rate for the foreground spectrum against the background one in the 2.4- to 2.8-MeV energy range as well as for the high-energy range up to 5.0 MeV (for the low-gain system). In Figs. 8 and 9 a noticeable maximum of the count rate in the 2.4- to 2.9-MeV interval is observed for both independent detectors as a result of subtracting background spectra from foreground spectra. The results obtained have a high level of confidence within this maximum (taken for 120 channels) and correspond to four to six standard deviations above the zero points (Figs. 8a and 8b). At the same time, for both detectors in the lower energy interval ($E < 2.3$ MeV), there are no significant results that could exceed the background level, while for the low-gain system, a broad additional band that is located between 3.0 and 5.0 MeV has been observed.

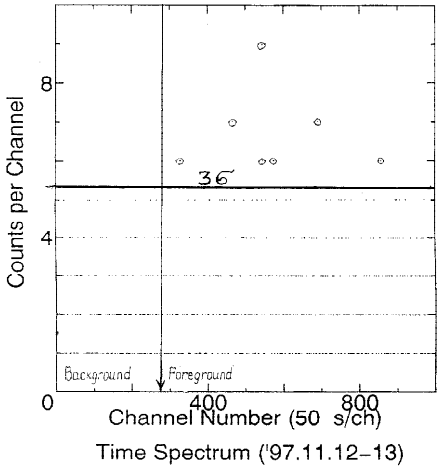

Fig. 6. Typical kinetics of neutron detection for a single experimental day; each channel corresponds to a 50-s duration.

In Figs. 9a and 9b, more detail is shown for the background subtraction within the 2.0- to 3.0-MeV energy interval for high- and low-gain systems for 20 channels. A clear maximum is apparent for both systems with the 2.5 ± 0.1 MeV position that within the calibration error we can ascribe to D-D neutrons ($E = 2.45$ MeV). The average count rates of the D-D neutron emission calculated as a statistical sum of counts inside the 2.5-MeV peaks were $\langle \Delta N \rangle_1 = (9.50 \pm 1.06) \times 10^{-4}$ counts/s (560 to 800 ch or 2300- to 2850-keV interval in Fig. 9a) for system 1 and $\langle \Delta N \rangle_2 = (7.20 \pm 1.28) \times 10^{-4}$ counts/s (1260 to 1410 ch or 2300- to 2900-keV interval in Fig. 9b) for system 2. One can see that these count rate values are close to one another. The mean count rate for two independent neutron detectors was, therefore, $\langle \Delta N \rangle = (8.35 \pm 0.82) \times 10^{-4}$ counts/s, or taking into account the total efficiency of the detection system, the intensity of D-D neutron emission in 4π solid angle was

$$I_n = (1.85 \pm 0.18) \times 10^{-2} \text{ n/s} \ .$$

Note that the presence of the 2.5-MeV peak in this case is not accompanied by a broad continuum from the low-energy side, as would be expected for the higher-intensity D-D neutron production. The absence of such a continuum could be attributed to the low intensity of

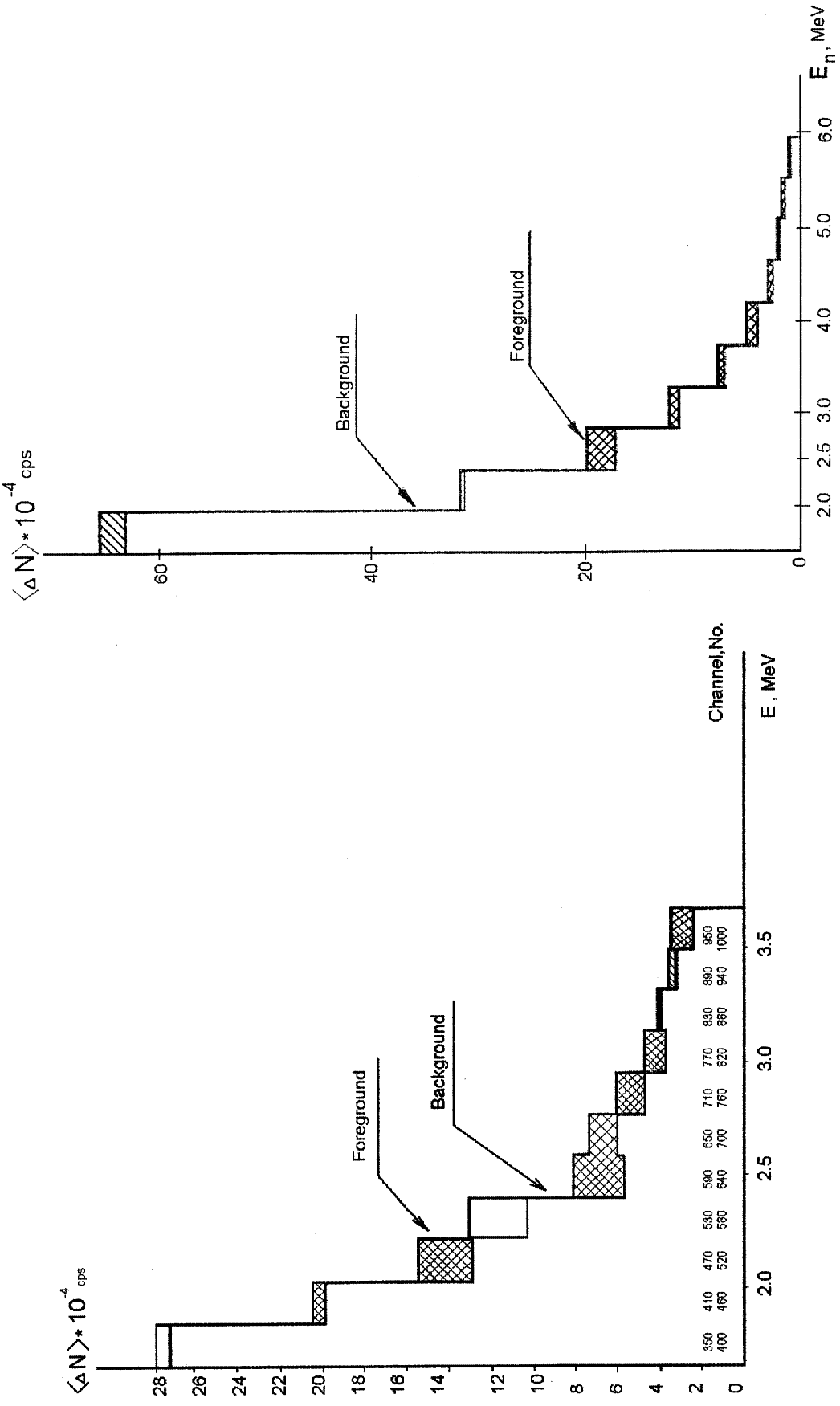

Fig. 7. Total neutron spectrum produced in all foreground and all background runs: (a) for system 1 and (b) for system 2. The number of channels here corresponds to neutron energy.

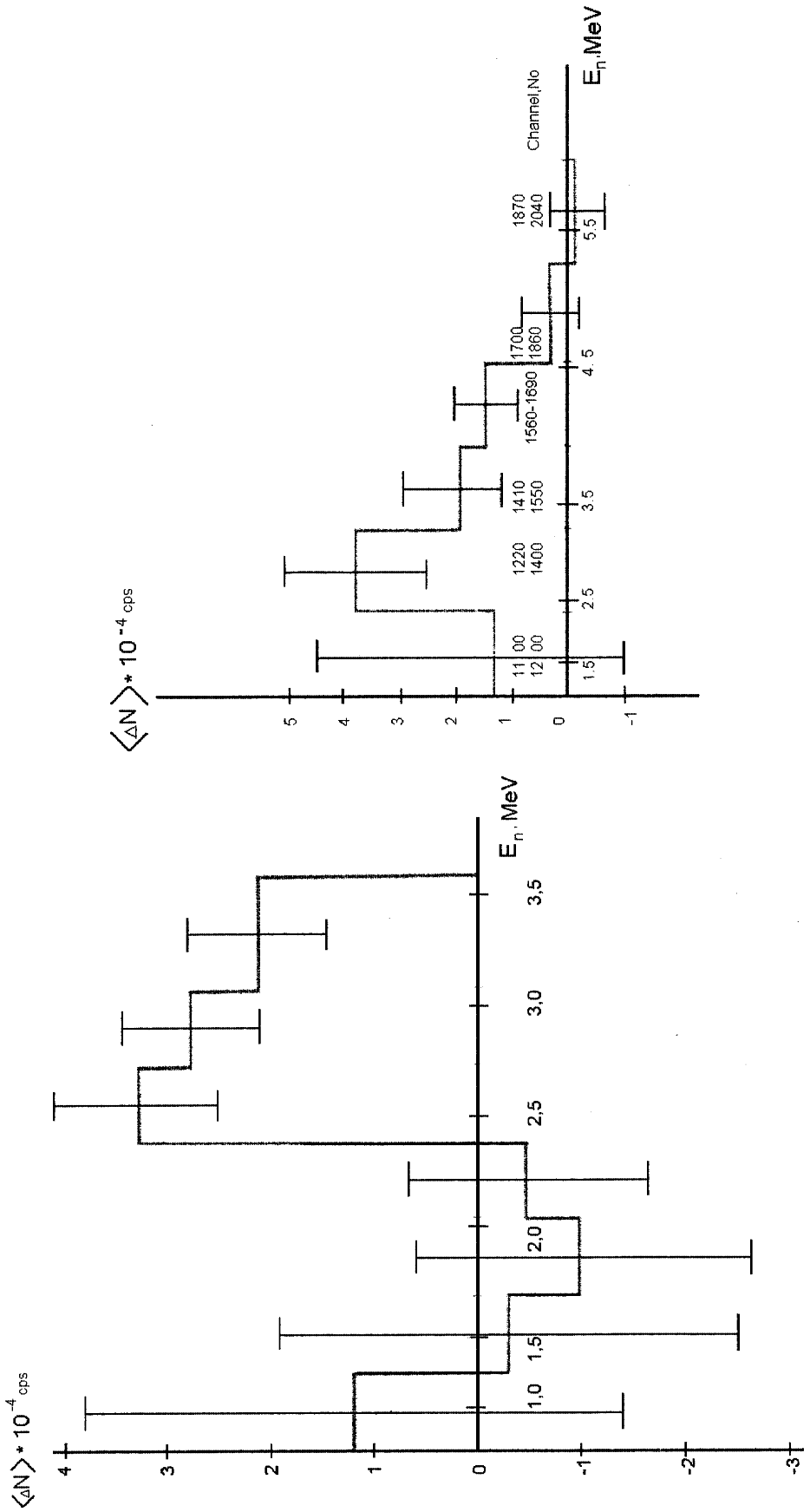

Fig. 8. Total difference between the sums of all foreground and background neutron spectra (with full statistical treatment) taken for 120 channels: (a) for system 1 and (b) for system 2.

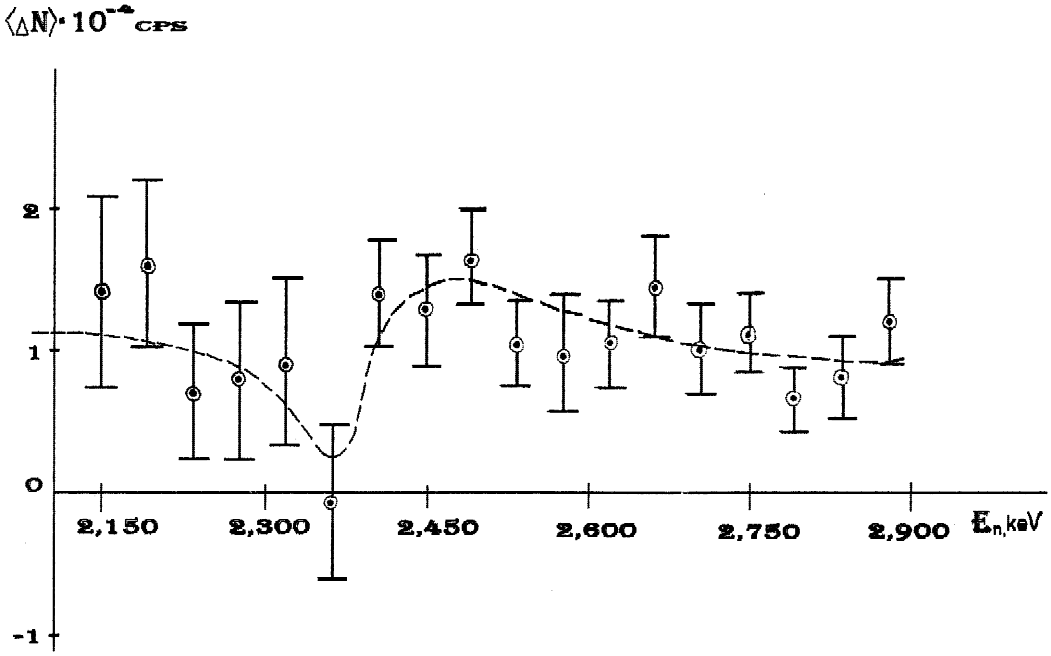

(a)

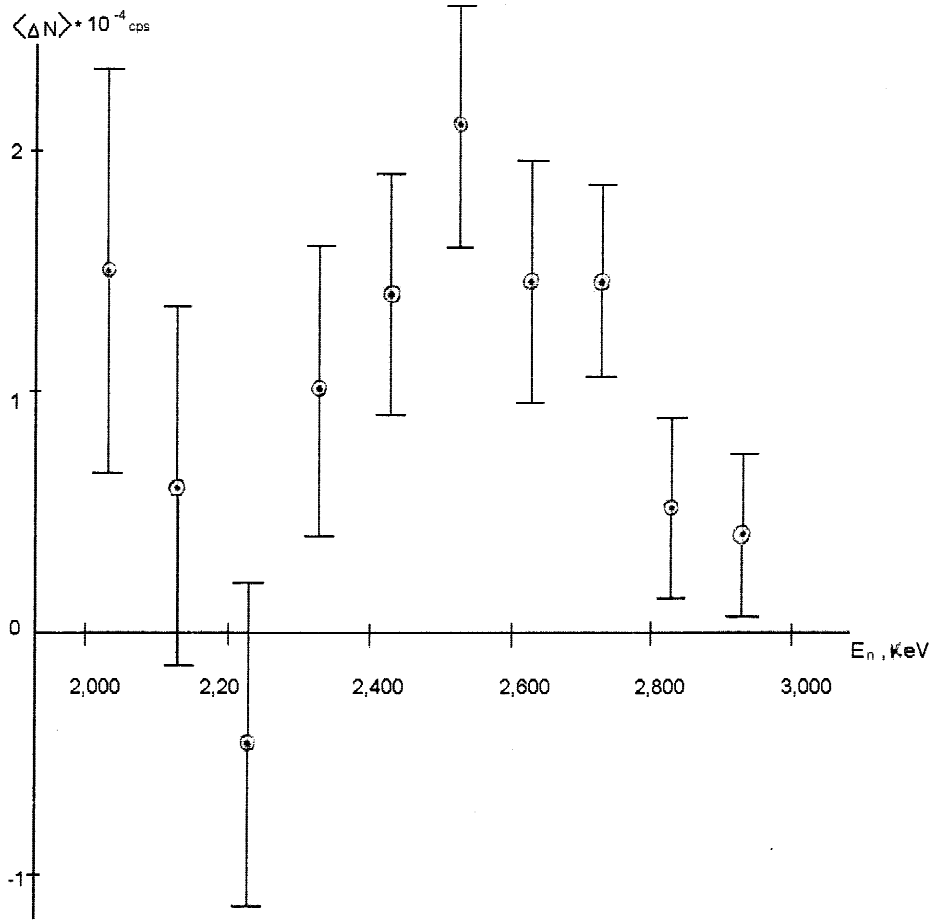

(b)

Fig. 9. Difference between the sums of all foreground and background neutron spectra within the 2.0- to 3.0-MeV energy interval taken for 20 channels: (a) for system 1 and (b) for system 2.

neutron emission observed. When the background count rate at $E < 2.0$ MeV is sufficiently high due to features of the response function (proton recoil spectra) of the NE-213 (Fig. 7a), it would be impossible to observe essential excess above the background in the neutron energy interval that is located below the 2.5-MeV peak position at very weak emission intensity. On the other hand, the broad continuum from the high-energy side, observed usually for D-D neutrons,[19] exists and extends to 5.0-MeV neutron energy (Figs. 8 and 9b) due to the low-background level of NE-213 at $E > 3.0$ MeV (Fig. 7b).

To estimate the influence of the mechanical strain on intensity of neutron emission, additional experiments with the same samples have been carried out in the absence of external plastic deformation ($\tau_f \sim 2 \times 10^5$ s). In this case, after subtracting background data in the energy interval of interest (2.0 to 3.0 MeV), the effect was only $\langle \Delta N \rangle' = (2.00 \pm 1.78) \times 10^{-4}$ counts/s, i.e., close to zero within the experimental error. Moreover, the maximum near 2.5 MeV for unstrained samples was not observed as well as in neutron time distribution (Fig. 6). There are no events that exceed a 3σ background level.

Therefore, data obtained allow a definite conclusion about actual observation of D-D neutron ($E = 2.45$ MeV) generation in the process of the exothermic D desorption in a mechanically strained Au/Pd/PdO:D heterostructure. Note that, in fact, the influence of random background fluctuations and distortion of spectral data (due to difference in foreground and background neutron scattering inside the experimental setup) have been excluded in our work, owing to the use (first time in an LINR study) of two independent high-efficiency NE-213 detectors in a low-background condition and blank Au/Pd/PdO samples, quite identical to the foreground one, but loaded with H.

III.B. Charged-Particle Measurements

III.B.1. SSB Detection Results

The total foreground spectrum for charged-particle detection is presented in Fig. 10a. From this figure one can see that the character of charged-particle counts as a function of particle energy is essentially different in experiments with Au/Pd/Pd:D heterostructure and in the background with the Au/PdO/Pd:H system (Fig. 10b) as well as in a long run with an empty sample (Fig. 4). In a background-run spectrum (Fig. 10b), the counts corresponding to the 2.0- to 3.0-MeV energy range are almost completely absent. This result is very close to data obtained for long-term background measurements (Fig. 4) in which the count rate in the energy interval under consideration is very low. In the same time, for the foreground spectrum in the 2.0- to 3.0-MeV energy interval, the number of events is considerably higher than in the background one.

The result of subtracting the Au/Pd/PdO:H data from that for Au/Pd/PdO:D and taking into account full statistical treatment is presented in Fig. 11. The excess under background runs takes place only in the 1- to 3-MeV energy interval with a clearly pronounced statistically significant maximum between 2 and 3 MeV. Note that for charged-particle emission, due to very low background and relatively short time (compared to neutron detection) of measurement at Osaka University, the statistics collected are several times lower than for neutrons. However, the total result for the 1.0-to 3.0-MeV interval after subtracting Au/Pd/PdO:H background is statistically significant:

$$\langle \Delta N_p \rangle = (1.46 \pm 0.40) \times 10^{-4} \text{ counts/s} \ .$$

Taking into account the detection efficiency in reference to alphas from an ^{241}Am source, we obtain the intensity for D-D proton emission in the 4π solid angle:

$$I_p = (4.0 \pm 1.0) \times 10^{-3} \text{ protons/s} \ .$$

Here, to estimate the total D-D proton yield, we used the entire energy interval of 1.0 to 3.0 MeV taking into account the opportunity for protons to escape from the bulk of the heterostructure, i.e., not only within the subsurface layer but also from a depth of ~1 to 10 μm that is possible during spontaneous heterostructure deformation and D moving between the PdO surface and the opposite side (Au coating).[13] In this case, the escaped protons would lose ~0.1 to 2.0 MeV in accordance with their stopping range in Pd metal.[22] In reference to our estimation for the most probable proton energy corresponding to the 2.0- to 3.0-MeV interval, the mean depth of escaping protons must be located in the layer at 1.0 to 6.0 μm from the surface. This makes the D-D proton detection in the Au/Pd/PdO:D heterostructure more difficult and less reproducible than neutron detection due to inevitable losses of proton flux inside the sample if the sample's thickness is higher or comparable to the 3-MeV proton stopping range in Pd.

To verify the assumed D-D proton energy losses in the sample, a specified experiment with heterostructures of different thickness has been carried out. As Fig. 12 shows, the 3.0-MeV proton count rate for Au/Pd/PdO:D samples strongly depend on the heterostructure thickness (h). Thus, statistically significant excess above the background level in the 2.5- to 3.5-MeV energy interval has been observed only for samples with thickness $h \leq 60$ μm. For the thick heterostructure samples ($h \geq 100$ μm), the count rate in the vicinity of 3.0 MeV is completely within the 3σ corridor of background error. One can see that thickness dependence of the 3.0-MeV proton yield is satisfactorily described by the usual logarithmic function. This fact confirms that the intensity of 3.0-MeV proton emission in Au/Pd/PdO:D samples actually depends on D diffusion (exponential dependence) through the heterostructure.

In fact, the subsurface layer of any sample should be almost empty of deuterons because the surface D is rapidly

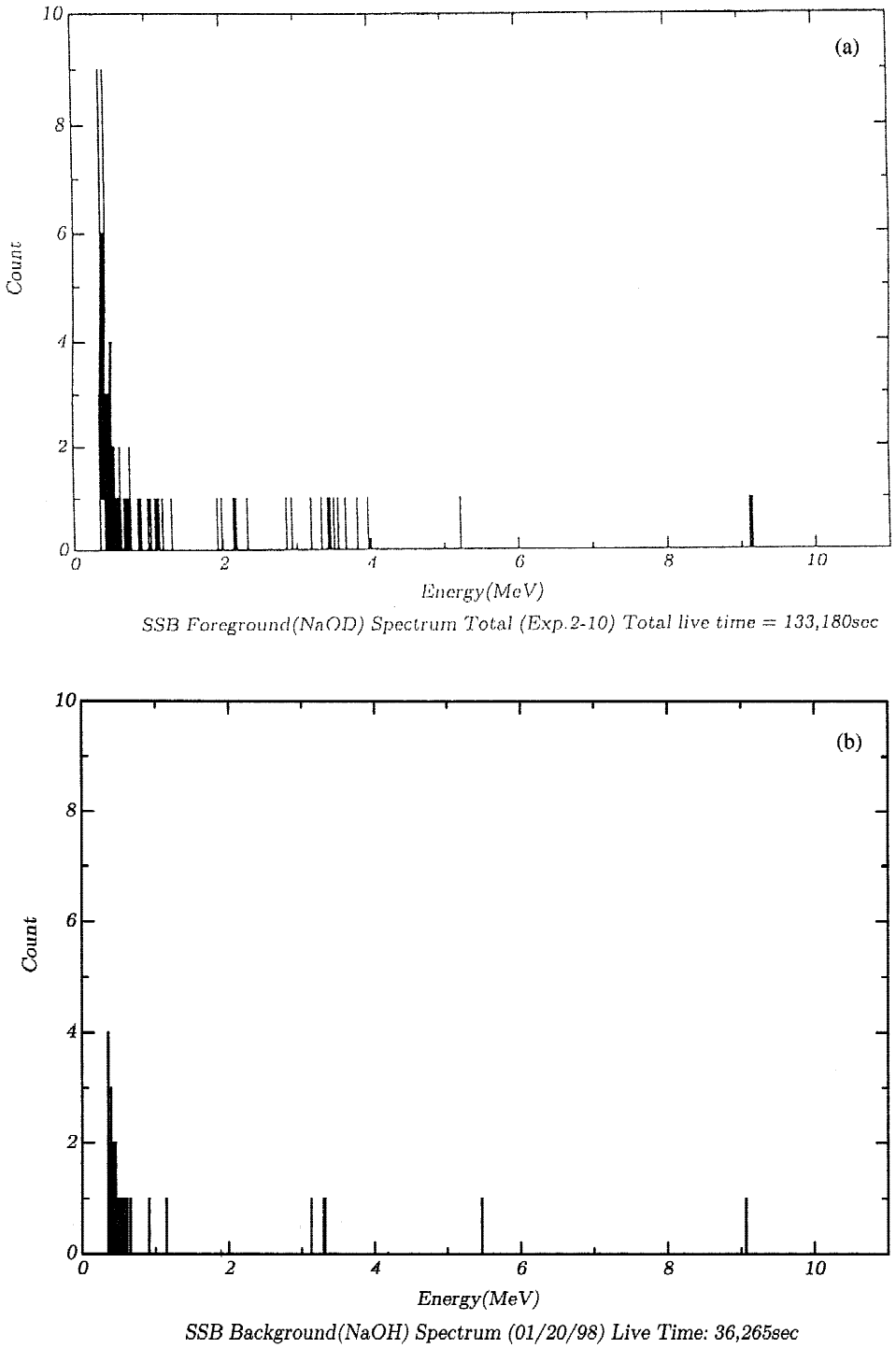

Fig. 10. Total (a) foreground spectrum for charged particles from 40- to 60-μm-thick Au/Pd/PdO:D samples in a vacuum and (b) background charged-particle spectrum obtained with 40-μm-thick Au/Pd/PdO:H samples in a vacuum.

recombined or desorbed just before exposure at the SSB detector (for instance, during pumping). It implies that D-D proton emission cannot be initiated in the subsurface layer, and protons escape from a certain depth of the sample. In this case, the effective depth for the 3.0-MeV proton escape increases with sample thickness owing to D diffusion between Pd/PdO interfaces from both sides of the sample. The diffusion stimulated by mechanical strain is more rapid in the thin samples, while in the thick samples, it is very slow[23] and the D concentration near

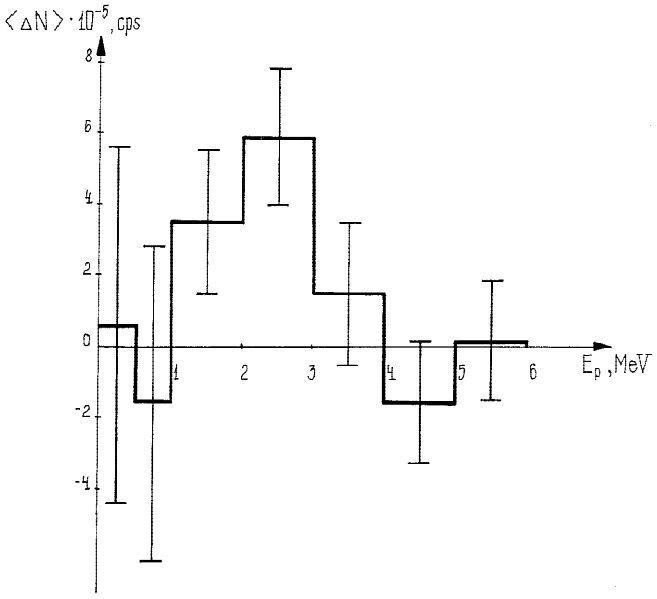

Fig. 11. Total difference between all foreground and background runs (with full statistical treatment) for charged-particle emission.

the surface is negligibly low. Therefore, the probability for D presence at a short distance from the surface in thin samples is much higher than in the thick ones. In this connection, for samples with $h > 60$ μm, according to our data, the effective depth of proton escape has to be >5 μm, and that is why 3.0-MeV protons cannot be observed.

III.B.2. CR-39 Detection Results

In the search for pt events with the foreground CR-39 detector ($S = 4.1$ cm^2) irradiated in experiment with the Au/Pd/PdO:D heterostructure, $N_f = 100$ double pt-like tracks were found, satisfying Fig. 5b. In the control (blank) detector ($S = 2.0$ cm^2), which was in contact with the Au/Pd/PdO:H sample for the same time interval as the foreground sample, $N_b = 8$ pt-like events were found. The background CR-39 detector ($S = 2.0$ cm^2) that was in contact with the empty (unloaded) Au/Pd/PdO sample has also demonstrated 8 pt-like events. This means that H does not contribute to pt tracks compared to the empty Au/Pd/PdO sample, where pt-like events observed are obviously caused by cosmic radiation and/or specific structural defects of the CR-39 subsurface layer. At the same time, our data in the foreground experiment with Au/Pd/PdO:D show an excess of pt track density six times above both the background and control runs. After subtracting background, the density of pt tracks generated in the thin subsurface layer of the heterostructure during the foreground sample exposure was $\Delta N_{pt} = (20.3 \pm 4.0)$ cm^{-2}. Taking into account the efficiency of

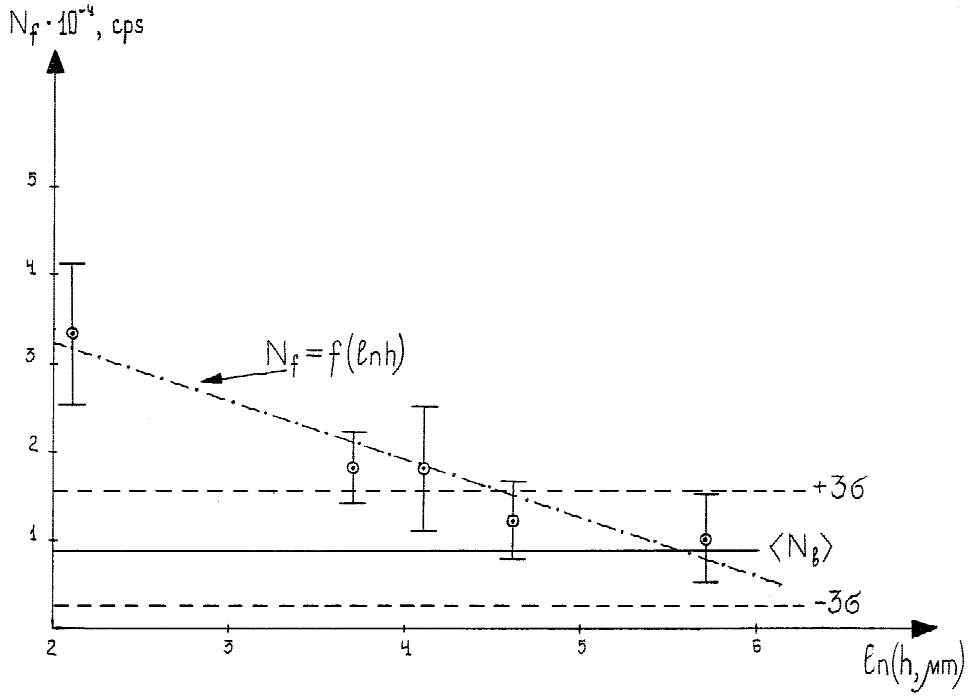

Fig. 12. Thickness dependence for the charged-particle count rate in the 2.5- to 3.5-MeV energy interval for 8- to 300-μm Au/Pd/PdO:D samples (measured with a 900-mm^2 SSB detector in a vacuum). The average background level (dashed line) corresponds to measurement with 40- to 100-μm Au/Pd/PdO:H samples.

pt event detection with CR-39 ($\epsilon_{pt} = 4.7\%$) and the total time of sample exposure ($t_{exp} = 7.2 \times 10^4$ s), we obtain the mean rate of protons and tritons generated in the D-D reaction in the Au/Pd/PdO:D heterostructure:

$$n_{pt} = (5.9 \pm 1.1) \times 10^{-3}\ \text{s}^{-1}, \text{ in } 4\pi \text{ solid angle} .$$

Note that the mean intensity of 3.0-MeV proton and 1.0-MeV triton emission for CR-39 charged-particle detection is only three times less than the 2.5-MeV neutron emission rate, obtained also in the air atmosphere with 40- to 60-μm Au/Pd/PdO:D samples under mechanical strain. On the other hand, it is important that the proton emission detected in the CR-39 experiment with 30-μm heterostructure samples is the same order of magnitude as that observed in SSB detector measurement in a vacuum. Therefore, we can conclude that the existence of the D(d, p)T reaction in Au/Pd/PdO:D heterostructure samples due to exothermic D desorption is confirmed by two independent detection techniques.

IV. CONCLUSIONS

We have observed a very low-intensity D-D reaction at a significant level by detection reaction products in both D$(d, n)^3$He and D(d, p)T channel products with close total intensities of $\sim$(4 to 19) $\times 10^{-3}$ particles/s. The lower level of proton emission compared to neutron emission in our experiments is satisfactorily explained by the absorption of charged particles during their escape from the bulk of a thick sample (40 to 60 μm), whose thickness is several times greater than the stopping range of 3.0-MeV protons in Pd.

The data obtained allow estimation of an average D-D reaction rate per D-D pair in the Au/Pd/PdO:D heterostructure due to exothermic D desorption. Taking into consideration the average deuteron concentration in the sample for foreground runs ($N_d = 1.0 \times 10^{20}$ D/cm^2 of heterostructure) and the mean D-D reaction yield in accordance with our experimental data, we obtain the mean rate of the D-D reaction in the Au/Pd/PdO:D sample: $\lambda_{dd} \sim 10^{-23}$ s^{-1} per D-D pair. This D-D reaction rate is much lower than was claimed for the excess heat production and could be comparable to the so-called Jones level.[2]

The mean rate of the D-D reaction obtained in the present study is at least two orders of magnitude lower than was estimated in previous works,[12,13] where a proportional BF_3 thermal neutron detector was used. Here, we try to show that the difference between the reaction yield in this work and in Ref. 13, taken per deuteron pair, actually, is nonexistent. The mean rate of the D-D reaction (λ_{dd}) derived is usually quite similar to Ref. 2, where λ has been determined as the ratio between the neutron count rate and the total D concentration in the crystalline lattice of the sample used. However, according to recent data,[15] large enhancement of the D-D reaction in metals under low-energy deuteron bombardment has been observed only for systems with high D mobility, in particular, for the Au/Pd/PdO heterostructure. In this connection, we can suggest estimating the D-D reaction yield in Au/Pd/PdO:D experiments using only a change in "mobile" D concentration. With mobile D it is possible to consider the deuterons that are desorbed from the sample during experiment. Let us consider the D-D reaction yield in terms of mobile D for two cases: the present experiment and an experiment[12,13] with similar electrochemically loaded Au/Pd/PdO:D samples that were tested in the regime of fast spontaneous thermal D desorption, similar to Ref. 11:

1. The change in mobile D concentration N_m(D) can be estimated, on average, using measurement of the D concentration in the sample N(D) before and after compression in the foreground run (Fig. 2). Before neutron detection (after electrochemical loading), $N^1(\text{D}) = 1.1 \times 10^{20}$ D/cm^2; after finishing the foreground run with compression, $N^2(\text{D}) = 7.0 \times 10^{18}$ D/cm^2. The sample's area is $S = 9.0$ cm^2. So, the mean rate of D desorption, taking into account foreground time $\tau = 3.6 \times 10^4$ s (Fig. 2) is $N_m(D) \approx N^1(\text{D})S/\tau = 2.5 \times 10^{16}$ D/s. And the D-D reaction yield with respect to 2.5-MeV neutrons, having intensity $I_n = 0.02$ n/s in 4π solid angle, is $R = 1.6 \times 10^{-18}$ reaction per D-D pair.

2. For this case, neutron detection has been carried out with a BF-3 proportional detector (without neutron energy analysis) during fast thermal desorption of D accompanied by spontaneous plastic deformation of the sample.[12] In accordance with Ref. 13, parameters of the experiment were as follows: $N^1(\text{D}) = 1.1 \times 10^{20}$ D/cm^2, $N^2(\text{D}) \le 10^{17}$ D/cm^2, $S = 4.0$ cm^2, and the time of thermal desorption of D is $\tau = 300$ s. The neutron emission intensity was $I_n = 0.92$ n/s. Then we have $N_m(\text{D}) = 1.3 \times 10^{18}$ D/s per sample and $R = 1.4 \times 10^{-18}$ reaction per D-D pair. At the same time, estimation of the D-D reaction rate λ_{dd} for total (initial) D concentration in the sample during experiment yields $\lambda_{dd} \sim 2 \times 10^{-21}$ s^{-1} per D-D pair.

As one can see, the yields of D-D reaction with respect to mobile D for cases 1 and 2 are close to one another. We can conclude that in both experiments, despite different experimental conditions, D-D neutrons were observed as a product of mobile deuteron fusion. Thus, in fact, a contradiction between present and previous[12,13] results does not exist.

In spite of the low intensity of the nuclear emissions obtained, we suppose that our data could be a proof of LINRs in deuterated solids stimulated by exothermic D desorption, because in background similar Au/Pd/PdO:H samples and similar conditions were used. Therefore, we conclude that emissions observed in Au/Pd/PdO:D samples can appear only due to D occurrence in a crystalline lattice where the count rates of D-D neutrons and protons become considerably higher than for background.

The possible nature of such a lattice-induced nuclear phenomenon may be considered to generate multiphonon excitation as a means of elastic energy transformation[10] and/or high electron (mobile deuteron) screening[24] that leads to anomalously large D-D reaction enhancement[15] in a Au/Pd/PdO:D heterostructure.

ACKNOWLEDGMENTS

This work was performed as a part of the New Hydrogen Energy Project of the New Energy Development Organization (NEDO), Japan.

The authors are grateful to J. Kasagi for his help in CR-39 calibration as well as to M. Okamoto, K. Matsui, A. V. Strelkov, P. Tripodi, M. Miles, and G. I. Merzon for fruitful discussions. The authors also thank H. Kamimura, T. Senju, E. Kennel, and Y. Isobe for their help in the preparation of certain experiments.

REFERENCES

1. B. V. DERJAGUIN et al., *Nature*, **341**, 492 (1989).

2. S. E. JONES et al., *Nature*, **338**, 737 (1989).

3. E. BOTTA et al., *Nuovo Cimen.*, **105A**, 1662 (1992).

4. E. STORMS, *J. Alloy Comput.*, **268**, 89 (1998).

5. Y. FUKAI and N. OKUMA, *Phys. Rev. Lett.*, **73**, 1640 (1995).

6. G. SHANI, C. COHEN, A. GRAEVSKY, and S. BROKMAN, *Solid State Com.*, **72**, 53 (1989).

7. A. G. LIPSON and D. M. SAKOV, *Rus. J. Tech. Phys. Lett.*, **20**, 46 (1994).

8. A. G. LIPSON, D. M. SAKOV, and E. I. SAUNIN, *JETP Lett.*, **62**, 828 (1995).

9. G. F. CEROFOLINI, G. BOARA, S. AGOSTEO, and A. F. PARA, *Fusion Technol.*, **23**, 465 (1993).

10. P. L. HAGELSTEIN, *Hyperfine Interact.*, **92**, 1059 (1994).

11. E. YAMAGUCHI and T. NISHIOKA, *Jpn. J. Appl. Phys.*, **29**, L666 (1992).

12. A. G. LIPSON, B. F. LYAKHOV, D. M. SAKOV, and B. V. DERJAGUIN, *Rus. J. Tech. Phys. Lett.*, **18**, 58 (1992).

13. A. G. LIPSON, B. F. LYAKHOV, and D. M. SAKOV, *Rus. J. Tech. Phys.*, **66**, 174 (1995).

14. A. S. ROUSSETSKI, *Progress in New Hydrogen Energy*, Vol. 1, p. 345, The Institute of Applied Energy, Tokyo, Japan (1996).

15. H. YUKI et al., *JETP Lett.*, **68**, 785 (1998).

16. H. YUKI et al., *J. Phys. G: Nucl. Part. Phys.*, **23**, 23 (1997).

17. U. GREIFE et al., *Z. Phys. A*, **351**, 107 (1995).

18. A. A. NAQVI, *Nucl. Instrum. Methods A*, **325**, 574 (1993).

19. F. ULKHAQ et al., *Radiat. Effects Defects Solids*, **115**, 135 (1990).

20. K. ODA et al., *Nucl. Instrum. Methods B*, **35**, 50 (1988).

21. G. F. KNOLL, *Radiation Detection and Measurement*, 2nd ed., J. Wiley, New York (1989).

22. H. H. ANDERSON and J. F. ZIEGLER, *Hydrogen Stopping Powers and Ranges in All Elements*, Pergamon Press, New York (1977).

23. Y. FUKAI and H. SUGIMOTO, *Adv. Phys.*, **34**, 263 (1985).

24. K. B. WHALEY, *Phys. Rev. B*, **41**, 3473 (1990).

Andrei G. Lipson (PhD, solid state physics, Institute of Physical Chemistry, Russian Academy of Sciences, Moscow, 1986) is a senior researcher, and a Vice Director of Laboratory of Physics of Active Surface at the Institute of Physical Chemistry, Russian Academy of Sciences. He is well known for his research on ferroelectrics, metal hydrides, electron excitation in solids, radiation physics of condensed matter, and low-energy nuclear processes.

Boris F. Lyakhov (MS, electric engineering, Moscow Energy Institute, 1963; PhD, electrochemistry, Institute of Physical Chemistry, Russian Academy of Sciences, Moscow, 1977) is a senior researcher in the Laboratory of Electrodeposition of Metals at the Institute of Physical Chemistry, Russian Academy of Sciences. His research interests are electrolysis, energy conversion in electrochemical processes, and diffusion of hydrogen in metals.

Alexei S. Roussetski (MS, experimental nuclear physics, Moscow Engineering Physics Institute, 1987; PhD, nuclear physics, Lebedev Physics Institute, Russian Academy of Sciences, 1999) is a scientific fellow in the Laboratory of Cosmic Rays at the Lebedev Physics Institute, Russian Academy of Sciences. His research interests are nuclear detection and lattice-induced nuclear reactions.

T. Akimoto, T. Mizuno, N. Asami, R. Shimada, S. Miyashita, A. Takahashi. Biographies not available at time of publication.